

Support information

Fe-N hollow mesoporous carbon spheres with high oxidase-like activity for sensitive detection of alkaline phosphatase

Yanwen Chen, Liu Zhao, Baoshuai Zhang, Yuqing Guan, Cheng Yao, and Xuan Xu *

*College of Chemistry and Molecular Engineering, Nanjing Tech University, Nanjing
211816, P. R. China*

* *Corresponding authors*

Fax: +86 25 58139527

E-mail addresses: xuxuan0205@njtech.edu.cn

Instruments

The morphologies and microstructures of porous carbons were characterized using a scanning electron microscope (SEM, Quanta FEG 250, USA) and a transmission electron microscope (TEM, Talos L 120C, USA). The nitrogen adsorption-desorption isotherms and Brunauer-Emmett-Teller (BET) surface areas of the materials were measured by a N₂ adsorption apparatus (Trister II 3020). A Tecnai TF-20 transmission electron microscopy with an attachment of the energy dispersive X-ray spectroscopy (EDS) was used to characterize the microstructure of the as-prepared catalysts and surface composition. Raman spectra was collected with a Labram HR800 Laser Raman spectrophotometer (Jobin Yvyon, France). X-ray photoelectron spectroscopy XPS analysis was carried out on an ESCALAB 250Xi (Thermo Scientific, USA) spectrometer with an Al K α radiation source. X-ray diffraction pattern (XRD) measurement was recorded at a Siemens D5000 X-ray diffraction meter using Cu K α radiation. UV–vis absorption spectroscopy was used to test on a TU-1900 double-beam UV–vis spectrophotometer (Persee, Beijing, China). Electron spin resonance (ESR) spectra was characterized by a Bruker A300 spectrometer (Germany). Inductively Coupled Plasma Optical Emission Spectrometry (ICP-OES) was characterized by an ICAP-7000 (Agilent, American).

Specific Activity

The specific activity (SA) of Fe-N HMCS and HMNCS were verified by color change using TMB as the chromogenic substrate. Various concentrations of Fe-N HMCS and HMNCS were added to the mixture, including 1.80 mL of HAc-NaAc (0.05 M, pH 3.5) and 100 μ L of TMB (10 mM), and the final absorbance was measured at 652 nm.

$$SA = \frac{V}{\varepsilon \times l} \times \left(\frac{\Delta A}{\Delta t} \right) \times m$$

V is the total volume of the reaction solution (μ L); ε is the molar absorption coefficient of the colorimetric substrate, which is typically maximized at 39,000 M⁻¹cm⁻¹ at 652 nm for TMB; l is the path length of light traveling in the cuvette (cm); A is the absorbance after subtraction of the blank value, and $\Delta A/\Delta t$ is the initial rate of change

in absorbance at 652 nm min^{-1} ; m is the nanozyme weight (mg) of each assay.

Monitoring of $\text{O}_2^{\cdot-}$, $\cdot\text{OH}$ and $^1\text{O}_2$ species

DMPO was used as the spin trapping agent to test $\cdot\text{OH}$ and $\cdot\text{O}_2^-$ radicals. For the measurement of $\cdot\text{OH}$, 10 mg mL^{-1} HMNCS or Fe-N HMCS was mixed with 100 mM DMPO in pH 4.0 HAc-NaAc buffer solution (0.2 M). After 5 min , the resulting solution was extracted by quartz capillary tube and placed in a glass tube for EPR analysis. The same process was used for $\text{O}_2^{\cdot-}$ radical measurement except that HMNCS or Fe-N HMCS was dispersed in methanol. Similar with $\cdot\text{OH}$ radical measurement, $^1\text{O}_2$ radicals were measured by using TEMP as the spin trapping agent while other conditions were the same.

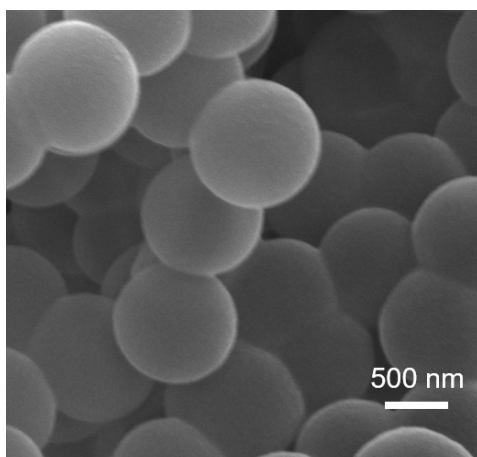


Fig. S1. SEM image of HMNCS.

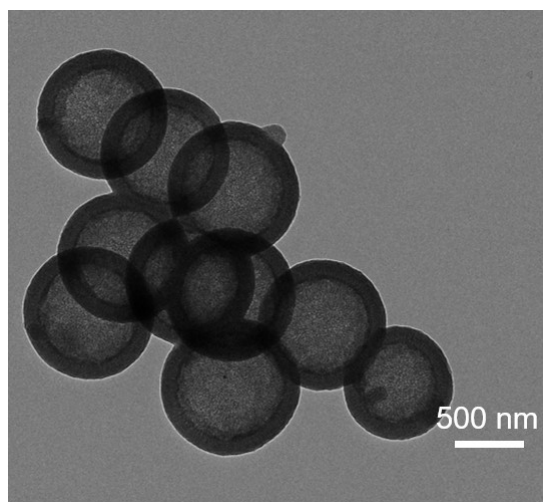


Fig. S2. TEM image of HMNCS.

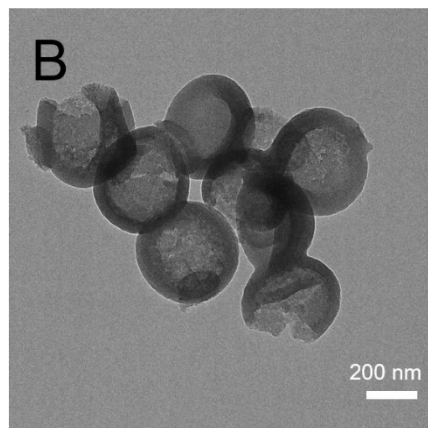
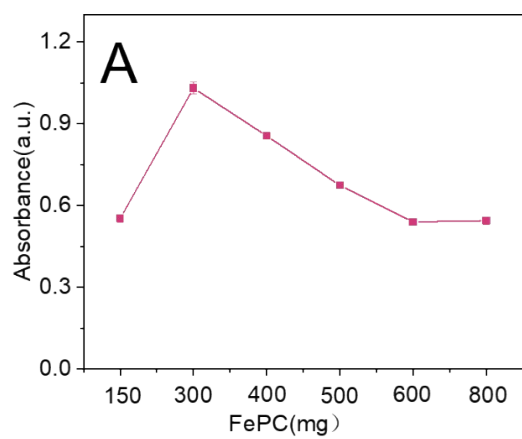


Fig. S3. (A) UV absorbance spectra of amount of FePC. (B) TEM image of Fe-N HMCS (FePC:600 mg).

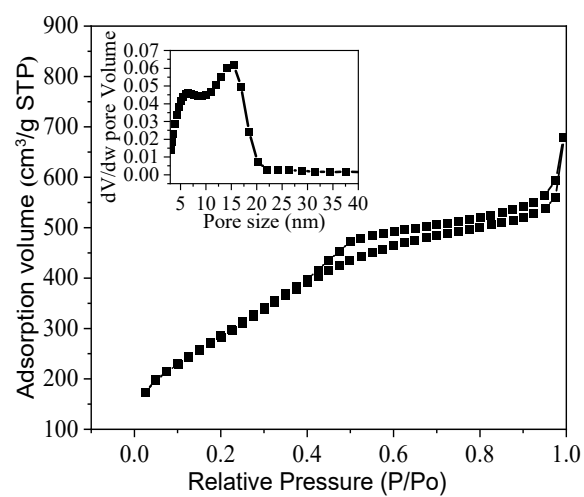


Fig. S4. N₂ sorption isotherms and pore size distributions (inset) of HMNCS.

Fig. S5. EDS spectrum of Fe-N HMCS.

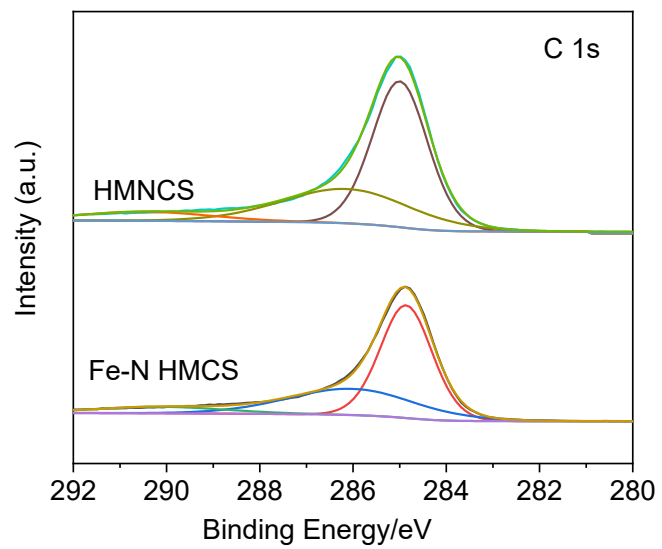


Fig. S6. C 1s of Fe-N HMCS and HMNCS.

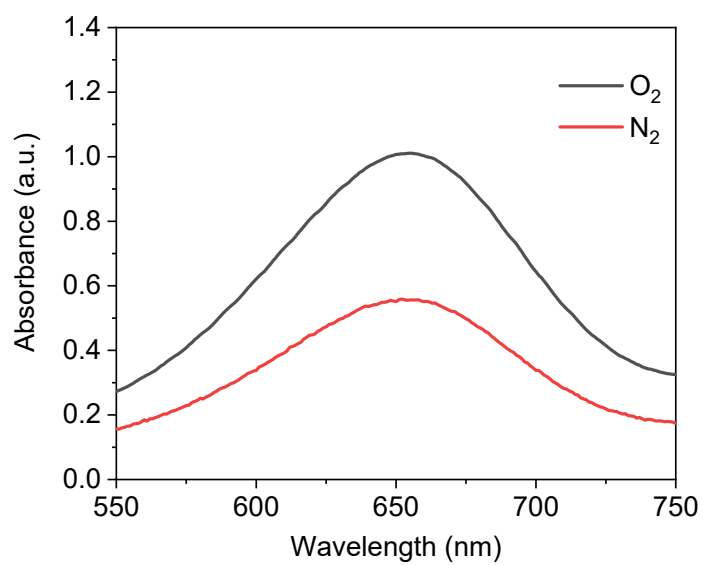


Fig. S7. UV absorbance spectra of the colorimetric reaction in N₂/O₂ saturated atmosphere.

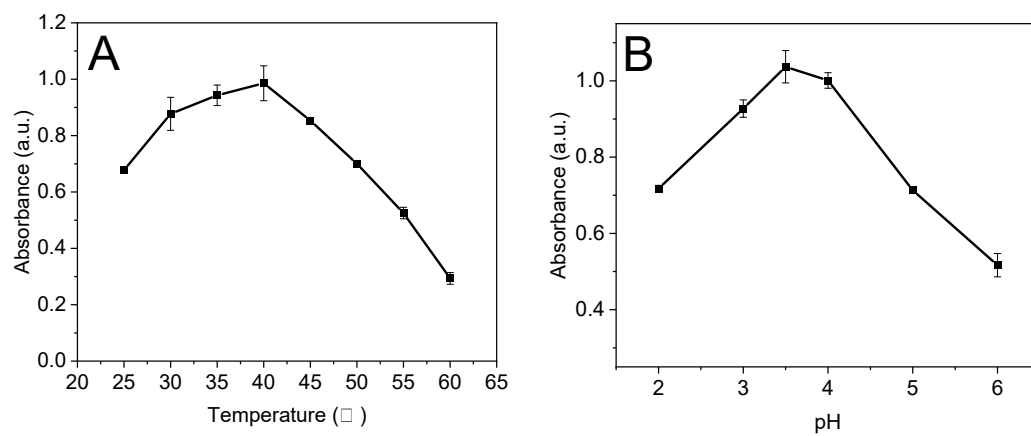


Fig. S8. (A) Temperature and (B) pH on the catalytic efficiency of Fe-N HMCS.

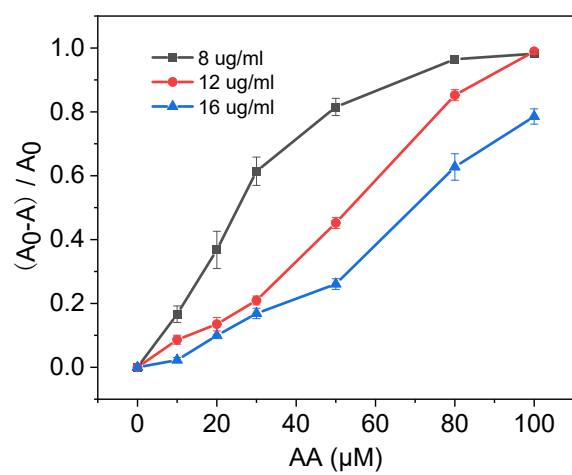


Fig. S9. Optimization of Fe-N HMCS concentration.

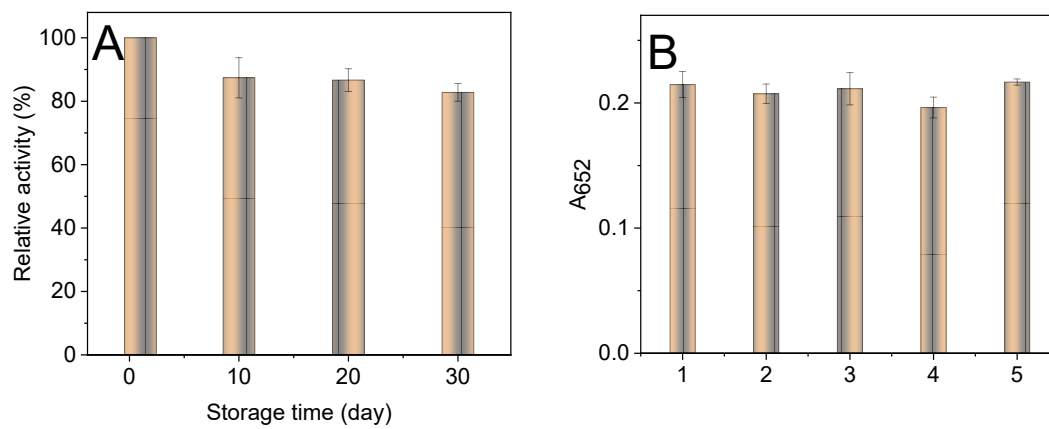


Fig. S10. (A) The catalytic activity of Fe-N HMCS for the period of 30-day storage. (B) Reproducibility of the Fe-N HMCS/TMB/AAP/ALP (20 U L^{-1}) sensing system.

Table S1. Kinetic parameters comparison of Fe-N HMCS with other oxidase-like nanozymes.

Catalyst	Substance	K_m (mM)	V_{max} (10^{-7} M s $^{-1}$)	Ref.
CeO ₂ NPs	TMB	0.42	1.00	[1]
CeO ₂ NPs	TMB	0.8-3.8	3.00-7.00	[2]
PAA-CeO ₂	TMB	0.60	0.31	[3]
MSN-AuNPs	TMB	0.22	1.19	[4]
Co ₃ O ₄ NPs	TMB	0.05	0.33	[5]
NiCo ₂ O ₄ MS	TMB	0.13	0.10	[6]
Se NPs	TMB	8.30	0.51	[7]
Fe-N/C-CNT	TMB	0.62	5.26	[8]
Fe SAEs	TMB	0.13	0.225	[9]
Fe-N HMCS	TMB	0.429	1.47	Our work

Table S2. Comparison of the current work with reported methods for the determination of ALP.

System	Method	Linear range (U/L)	LOD (U/L)	Refs
CdS QDs	Fluorescence	0-50	0.5	[10]
ICP ^a	Fluorescence	25-200	10	[11]
PDA NPs	Fluorescence	0-18	0.4	[12]
CQDs	Fluorescence	16.7-782.6	1.1	[13]
CdSe nanoparticles	Electrochemistry	2-25	2	[14]
FeCo NPs@PNC	Colorimetry	0.6-10	0.49	[15]
Cu(II)-phenanthroline	Colorimetry	0-200	1.25	[16]
Fe(II)-phenanthroline	Colorimetry	0-220	0.94	[17]
DNA-Cu(II) complexes	Colorimetry	20-200	0.84	[18]
PDA nano-liposomes	Colorimetry	10-200	2.8	[19]
Fe-N HMCS	Colorimetry	0.01-30	0.42	Our work

^a Infinite coordination polymer

Additional References

1. H. Cheng, S. Lin, F. Muhammad, Y.-W. Lin and H. Wei, *ACS Sensors*, 2016, **1**, 1336-1343.
2. A. Asati, S. Santra, C. Kaittanis, S. Nath and J. M. Perez, *Angew Chem Int Ed Engl*, 2009, **48**, 2308-2312.
3. S. X. Zhang, S. F. Xue, J. Deng, M. Zhang, G. Shi and T. Zhou, *Biosens Bioelectron*, 2016, **85**, 457-463.
4. Y. Tao, E. Ju, J. Ren and X. Qu, *Adv Mater*, 2015, **27**, 1097-1104.
5. W. Qin, L. Su, C. Yang, Y. Ma, H. Zhang and X. Chen, *J Agric Food Chem*, 2014, **62**, 5827-5834.
6. L. Su, W. Dong, C. Wu, Y. Gong, Y. Zhang, L. Li, G. Mao and S. Feng, *Anal Chim Acta*, 2017, **951**, 124-132.
7. L. Guo, K. Huang and H. Liu, *Journal of Nanoparticle Research*, 2016, 18: 1-10.
8. Y. Wang, Z. Zhang, G. Jia, L. Zheng, J. Zhao and X. Cui, *Chem Commun (Camb)*, 2019, **55**, 5271-5274.
9. C. Zhao, C. Xiong, X. Liu, M. Qiao, Z. Li, T. Yuan, J. Wang, Y. Qu, X. Wang, F. Zhou, Q. Xu, S. Wang, M. Chen, W. Wang, Y. Li, T. Yao, Y. Wu and Y. Li, *Chem Commun (Camb)*, 2019, **55**, 2285-2288.
10. N. Malashikhina, G. Garai-Ibabe and V. Pavlov, *Anal Chem*, 2013, **85**, 6866-6870.
11. J. Deng, P. Yu, Y. Wang and L. Mao, *Anal Chem*, 2015, **87**, 3080-3086.
12. D. E. Wang, S. You, W. Huo, X. Han and H. Xu, *Mikrochim Acta*, 2022, **189(2)**, 70.
13. Z. S. Qian, L. J. Chai, Y. Y. Huang, C. Tang, J. Jia Shen, J. R. Chen and H. Feng, *Biosens Bioelectron*, 2015, **68**, 675-680.
14. H. Jiang and X. Wang, *Anal Chem*, 2012, **84**, 6986-6993.
15. T. T. Wu, Z. Y. Ma, P. P. Li, M. L. Liu, X. Y. Liu, H. T. Li, Y. Y. Zhang and S. Z. Yao, *Talanta*, 2019, **202**, 354-361.
16. Q. Hu, M. He, Y. Mei, W. Feng, S. Jing, J. Kong and X. Zhang, *Talanta*, 2017, **163**, 146-152.
17. Q. Hu, B. Zhou, P. Dang, L. Li, J. Kong and X. Zhang, *Analytica Chimica Acta*, 2017, **950**, 170-177.
18. J. Yang, L. Zheng, Y. Wang, W. Li, J. Zhang, J. Gu and Y. Fu, *Biosens Bioelectron*, 2016, **77**, 549-556.
19. J. X. Tian, Y. Z. Fang, R. Yu, Z. Y. Zhang, Y. T. Zhuo, J. Y. He, S. Wu, Q. Xiao and X. J. Kong, *Anal Methods*, 2021, **13**, 322-326.